Mechanisms of the Shape Evolution of CdSe Nanocrystals

Z. Adam Peng and Xiaogang Peng*

Contribution from the Department of Chemistry and Biochemistry, University of Arkansas, Fayetteville, Arkansas 72701

Received July 27, 2000

Abstract: The temporal shape evolution of CdSe quantum confined nanorods (quantum rods) in nonaqueous solvents with organometallic precursors was studied quantitatively and systematically. The experimental results revealed three distinguishable stages in the shape evolution. At high monomer concentrations, nanocrystals grow exclusively along the *c*-axis of the wurtzite structure, making this axis the long axis of the rods. At intermediate concentrations, nanocrystals grow simultaneously in three dimensions. At low monomer concentrations, the aspect ratio decreases in a process controlled by intraparticle diffusion on the surface of the nanocrystals. This intraparticle ripening stage is different from normal Ostwald ripening, which occurs at lower monomer concentrations and is by monomer migration from small to larger ones. Addition of hexylphosphonic acid or tetradecylphosphonic acid, strong cadmium ligands, is important mainly because it enables the high monomer concentrations needed for the growth of quantum rods. A simple model is proposed to explain the growth of faceted CdSe nanocrystals on the basis of diffusion control.

Introduction

Colloidal inorganic nanocrystals are of great interest for both fundamental research and technical applications, due to their strong size and shape dependent properties and excellent chemical processibility.[1−4] In most cases, these advantages can be exploited only with relatively monodisperse samples. Control of nanocrystal shape is important in various applications, such as catalysis,[5] solar cells,[6] light-emitting diodes,[7,8] and biological labeling.[9,10] The simultaneous control of size, morphology, and size distribution of colloidal nanocrystals is a challenging topic. In fact, morphology control alone is already quite difficult. This is so because very little is quantitatively known about crystallization in general,[11,12] regardless of size and shape.

Several groups have reported shape-controlled synthesis of different types of colloidal nanocrystals. In some cases, information regarding the growth mechanism is reported as discussed below. The vapor−liquid−solid growth technique and its analogues have been used to produce nanowires by the use of nanosized liquid or solid "seeds".[13−16] In general, the size and aspect ratio distributions of these nanowires are hard to control, although the most recent work reported a reasonably narrow distribution of the diameter of the silicon nanowires, about 20% relative standard deviation.[13] In addition, reverse micelle and carbon nanotubes were used as templates to direct the growth of nanowires/nanorods.[17−19] Qian and his group hydrothermally synthesized a variety of nanowires by using ethylenediamine as a ligand.[20] Even though the mechanism was not well understood, these authors[20] discovered that this ligand was unique, and could not be replaced by pyridine or diethylamine for the preparation of nanowires. There are several examples of shape control for metal nanocrystal growth in solution without using a template.[5,21,22] Curtis et al.[22] hypothesized that the formation of copper hexagons in their system was due to the existence of a stable complex of copper ions. El-Sayed's group,[23] and later Reetz's group,[24] pioneered growth mechanism studies of the shape control for transition metal nanocrystals. Unfortunately they did not provide information on some of the important factors including the temporal variation of the monomer concentration in the growth solution. Both groups suggested that the shape control of transition metal nanocrystals observed was due to the presence of stabilizing reagents bound to the surface of nanocrystals.

(1) Peng, X. G.; Manna, L.; Yang, W. D.; Wickham, J.; Scher, E.; Kadavanich, A.; Alivisatos, A. P. *Nature* **2000**, *404*, 59−61.
(2) Heath, J. R., Ed. *Acc. Chem. Res.* **1999**, *32*, 1ff; special issue on nanostructures.
(3) Alivisatos, A. P. *Science* **1996**, *271*, 933−937.
(4) Brus, L. E. *J. Chem. Phys.* **1986**, *90*, 2555.
(5) Ahmadi, T. S.; Wang, Z. L.; Green, T. C.; Henglein, A.; Elsayed, M. A. *Science* **1996**, *272*, 1924−1926.
(6) Huynh, W.; Peng, X.; Alivisatos, A. P. *Adv. Mater.* **1999**, *11*, 923−927.
(7) Schlamp, M. C.; Peng, X. G.; Alivisatos, A. P. *J. Appl. Phys.* **1997**, *82*, 5837−5842.
(8) Mattoussi, H.; Radzilowski, L. H.; Dabbousi, B. O.; Thomas, E. L.; Bawendi, M. G.; Rubner, M. F. *J. Appl. Phys.* **1998**, *83*, 7965−7974.
(9) Bruchez, M.; Moronne, M.; Gin, P.; Weiss, S.; Alivisatos, A. P. *Science* **1998**, *281*, 2013−2016.
(10) Chan, W. C. W.; Nie, S. M. *Science* **1998**, *281*, 2016−2018.
(11) Oxtoby, D. W. *Acc. Chem. Res.* **1998**, *31*, 91.
(12) Mullin, J. W. *Crystallization*, 3rd ed.; Butterworth-Heinemann: Oxford, Boston, 1997.
(13) Holmes, J. D.; Johnston, K. P.; Doty, R. C.; Korgel, B. A. *Science* **2000**, *287*, 1471−1473.
(14) Morales, A. M.; Lieber, C. M. *Science* **1998**, *279*, 208−211.
(15) Dai, H. J.; Wong, E. W.; Lu, Y. Z.; Fan, S. S.; Lieber, C. M. *Nature* **1995**, *375*, 769−772.
(16) Trentler, T. J.; Hickman, K. M.; Goel, S. C.; Viano, A. M.; Gibbons, P. C.; Buhro, W. E. *Science* **1995**, *270*, 1791−1794.
(17) Li, M.; Schnablegger, H.; Mann, S. *Nature* **1999**, *402*, 393−395.
(18) Pileni, M. P. *Adv. Mater.* **1999**, *10*, 1358−1362.
(19) Han, W. Q.; Fan, S. S.; Li, Q. Q.; Hu, Y. D. *Science* **1997**, *277*, 1287−1289.
(20) Wang, W. Z.; Geng, Y.; Yan, P.; Liu, F. Y.; Xie, Y.; Qian, Y. T. *Inorg. Chem. Commun.* **1999**, *2*, 83−85.
(21) Yu, Y. Y.; Chang, S. S.; Lee, C. L.; Wang, C. R. C. *J. Phys. Chem. B* **1997**, *101*, 6661−6664.
(22) Curtis, A. C.; Duff, D. G.; Edwards, P. P.; Jefferson, D. A.; G., J. F.; Kirkland, S. I.; Wallace, A. S. *Angew, Chem., Int. Ed. Engl.* **1988**, *27*, 1530.
(23) Petroski, J. M.; Wang, Z. L.; C., G. T.; El-Sayed, M. *J. Phys. Chem. B* **1998**, *102*, 3316−3320.
(24) Bradley, J. S.; Tesche, B.; Busser, W.; Maase, M.; Reetz, M. T. *J. Am. Chem. Soc.* **2000**, *122*, 4631−4636.

10.1021/ja0027766 CCC: $20.00
Published on Web 01/30/2001

Compared to other types of colloidal nanocrystals, semiconductor nanocrystals are more suited for studying crystallization. Their strong size- and shape-dependent optical properties[1−3] can be used as convenient probes. For example, Vossmeyer et al. reported the growth kinetics of CdS nanocrystals in aqueous solution studied by monitoring the temporal evolution of the UV−vis absorption spectrum.[25] This was further demonstrated by Peng et al.[26] through the study of the growth kinetics of CdSe and InAs nanocrystals in nonaqueous solution at 280−360 °C. Using the unique band-edge photoluminescence of the nanocrystals, Peng et al. was able to quantitatively determine the average size and the size distribution of CdSe nanocrystals during their growth. Their experimental results demonstrate that the Gibbs−Thompson law, i.e. the solubility of crystals increases as the size of the crystals decreases, plays an important role in determining the growth kinetics of those nanocrystals. They observed that, if the monomer concentration in the solution is higher than the solubility of all existing nanocrystals, all nanocrystals in the solution grow and the size distribution narrows down. This is the "focusing of size distribution", which can be exploited for the spontaneous formation of close to monodisperse colloidal nanocrystals. The depletion of monomer by the growth of nanocrystals will eventually make the smaller nanocrystals in the solution soluble, due to the strongly size-dependent solubility in the nanometer regime. This means that the smaller nanocrystals in the solution shrink and the bigger ones continue their growth. As a result, the size distribution broadens. This is the "defocusing of size distribution" (Ostwald ripening) and should be avoided for formation of relatively monodisperse colloidal nanocrsytals. The focusing of size distribution can be due to either a diffusion-controlled process or the higher chemical reactivity of the smaller nanocrystals in the solution.

Peng et al. further explored the growth of CdSe nanocrystals under very high monomer concentrations and observed the formation of CdSe quantum rods.[1] Instead of relying on the impurities in technical grade trioctylphosphine oxide (TOPO), the authors at first used a mixed reaction solvent composed of high grade TOPO and hexylphosphonic acid (HPA), which is an analogue of a key impurity in technical grade TOPO. They reported that low HPA concentrations ($<5\%$ in mass) generated spherical CdSe nanocrystals and the growth kinetics was very similar to those described in the paragraph above. However, with high HPA concentrations ($\geq 5\%$), their conditions reproducibly yield CdSe quantum rods. The authors further discovered that, in the initial stage, CdSe nanocrystals can rapidly grow primarily along the *c*-axis of the wurtzite structure to form quantum rods. The control of the aspect ratio (up to 10) and aspect ratio distribution of these CdSe quantum rods was not as good as that of their short axis dimension which can be within 5−10% of the relative standard deviation. Shortly after this rod growth process, as the monomer depleted due to the rods growth stage, the aspect ratio of nanocrystals decreased to nearly one and the short axis grew significantly.

The authors did not provide detailed information regarding the mechanism of shape control for these CdSe quantum rods. In fact, we found that the high growth rate and the relatively broad aspect ratio distribution of CdSe quantum rods reported by Peng et al.[1] are not suited for a detailed and quantitative study of their growth mechanism. In the present work, we optimized the growth conditions by manipulating the composition of the reaction solvent, the stock solution, the reaction temperature, the injection methods, etc. The well-controlled growth rate and the relatively monodiserse quantum rods allowed a careful study of the parameters controlling shape evolution. Furthermore, we have developed a reliable method to determine the monomer concentration in the solution (see the first paragraph in Results section for the definition of monomers). We will identify below three distinguishable shape evolution stages, which are mainly determined by the monomer concentration in solution. These three stages include the two observed by Peng et al.,[1] i.e. the dominant rods growth and the shape evolution from rods to dots, and a new stage, involving quantum rods growing along all three dimensions. Furthermore, we found that the shape evolution from rods to dots occurs through an intraparticle monomer migration process. The results described below will also show that strong cadmium ligands are important in the shape control of quantum rods, mainly because they are needed to achieve high monomer concentrations in solution. Overall, the growth of CdSe nanocrystals is diffusion controlled and thus cannot be explained by the Gibbs−Curie−Wulff law,[12] which does not allow any shape evolution. The current results and others reported previously[1,26] can be explained by a simple model based on diffusion-controlled growth and the unique wurtzite structure of crystalline CdSe. Unlike the traditional diffusion theories of crystal growth,[12] the model proposed here allows crystals to possess a faceted shape. Applying the model makes it possible to obtain relatively monodisperse CdSe single crystalline quantum rods with a high aspect ratio.

Experimental Section

Chemicals. Dimethyl cadmium, $Cd(CH_3)_2$, was purchased from Strem Chemicals and vacuum transferred from its original cylinder to remove the impurities. The purified $Cd(CH_3)_2$ was stored in a refrigerator located inside a glovebox. Tributylphosphine (TBP), trioctylphosphine (TOP), 99% trioctylphosphine oxide (TOPO), hexylphosphonic dichloride, and Se powder were purchased from Aldrich. Methanol, toluene, and diethyl ether were purchased from VWR. Tetradecylphosphonic acid (TDPA) was purchased from Alfa. Hexylphosphonic dichloride was converted to HPA by reacting with water. The resulting HPA was purified by extraction with diethyl ether. Solid HPA was isolated by evaporation of the ether solution.

Stock Solutions. Two different types of CdSe stock solutions were used. The first one is a traditional one containing $Cd(CH_3)_2$ and Se dissolved in TBP or TOP developed by Murray et al. [27] The Cd:Se atom ratios varied from 1.5:1 to 1:1.3. Apart from this, separated stock solutions for $Cd(CH_3)_2$ and Se in TBP or TOP were also employed. The concentrations of the stock solutions were controlled to reach the initial Cd concentration in the reaction mixture being between 0.9% and 3.6% of cadmium element by mass.

Growth of CdSe Nanocrystals. Four grams of the mixture of TOPO mixed with known amounts of either HPA or TDPA were heated to 320−360 °C and used as reaction solvent. In the one-stock solution approach, two grams of the stock solution were rapidly injected into the hot solvent. For the two-stock solution approach, the cadmium stock solution was injected 10−60 s before the Se stock solution. The total mass of the two-stock solutions was 2 g for all the initial injections. The growth of quantum rods was carried out at a given temperature in the range of 250−300 °C after the injection. Nanocrystal growth was stopped by lowing the temperature to ambient. All procedures were carried out with standard air-free techniques. Since this work focuses on the study of the growth mechanism, no size separation was performed for any nanocrystal samples employed for measurements.

The growth by the one-stock-solution approach described here is similar to the ones reported by Peng et al.[1] A typical growth reaction

(25) Vossmeyer, T.; Katsikas, L.; Giersig, M.; Popovic, I. G.; Diesner, K.; Chemseddine, A.; Eychmuller, A.; Weller, H. *J. Phys. Chem.* **1994**, *98*, 7665−7673.

(26) Peng, X. G.; Wickham, J.; Alivisatos, A. P. *J. Am. Chem. Soc.* **1998**, *120*, 5343−5344.

(27) Murray, C. B.; Norris, D. J.; Bawendi, M. G. *J. Am. Chem. Soc.* **1993**, *115*, 8706−8715.

for the two-stock-solution approach was carried out as follows. The HPA/TOPO mixture with 8% HPA was heated to 360 °C. The Cd stock solution (0.162 g of $Cd(CH_3)_2$ + 0.340 g of TBP) was added into the hot HPA/TOPO mixture over about 10 s without significant variation of the temperature. After about 30 s, 1.5 g of the selenium/TBP solution was quickly injected at 360 °C. The Cd:Se atomic ratio was 1:1.3 and the growth temperature was set at 250 °C. After 20 min, a new cadmium stock solution (0.0303 g of $Cd(CH_3)_2$ + 0.120 g of TBP) was added dropwise into the reaction vessel. After an additional 2 min, a new selenium stock solution (0.0168 g of Se + 0.130 g of TBP) was added in the same manner. Such secondary injections were repeated 6 times in 4 h to maintain the free Cd concentration in solution in the range of 1.4−2% by mass.

Monitoring the Growth. The growth reactions were monitored by UV−vis absorption and photoluminescence spectra recorded with aliquots taken from the reaction flask at several time intervals after the initiation of a growth reaction. The needle-tip amounts of aliquots were immediately cooled to ambient temperature by mixing with about 0.5 mL of cold toluene after being taken from the reaction vessel. From each aliquot, thousands of nanocrystals were surveyed by transmission electron microscopy (TEM). High-resolution TEM and X-ray powder diffraction (XRD) were employed to check the crystallinity of nanocrystals. Statistical evaluations included all the nanocrystals in a chosen area of a TEM micrograph (about 500 ± 50 particles), excluding only crystals in undistinguishable aggregates (<5%). The volume of a given nanocrystal was approximated as the product of its long axis dimension times the square of its short axis dimension.

The Cd Monomer Concentration in Solution. The reaction mixture with approximately 0.2−0.4 mL was taken from the reaction flask at certain reaction time intervals. These aliquots were immediately precipitated in 3 mL of methanol. The mass of the aliquots was then determined by subtracting the mass of the methanol from the total mass of the methanol and the reaction aliquots. The precipitate was isolated by centrifugation and decantation and washed with methanol three times. The nanocrystals were then dissolved by toluene. An insoluble white solid was separated from the colored nanocrystals/toluene solution by centrifugation/decantation. The toluene solution was treated by methanol to precipitate CdSe nanocrystals. This purified nanocrystal precipitate was isolated by centrifugation/decantation and dried under vacuum. The nanocrystal powder was weighed prior to a standard HCl/HNO_3 digestion for Inductively-Coupled-Plasma atomic emission (ICP) measurements. The cadmium concentration in this digested solution was determined by ICP, and the Cd monomer concentration in the growth solution at a given moment is calculated by excluding the Cd in the form of nanocrystals from the total amount of Cd atoms added into the reaction flask.

Characterization of the Cadmium HPA (Cd−HPA) or Cadmium TDPA (Cd−TDPA) Complex. The white precipitate isolated from nanocrystal/toluene solution was washed three times by methanol. The final precipitate was then dried under vacuum. The mass of the dried precipitate was recorded before the digestion by HCl/HNO_3 aqueous solution. The organic phase of the digestion solution was extracted by ethyl ether and washed by pure water three times. After evaporation of ethyl ether, the white solid was characterized by ^{1}H NMR and mass spectroscopy. The cadmium concentration of the aqueous phase was measured by ICP.

Results

The determination of monomer concentration for a crystallization system is an essential step to fully define the system. In the current system, it is hard to determine the monomer concentration at the high reaction temperatures directly. Instead, we indirectly obtained this information by determining the number of Cd atoms in the form of nanocrystals. At this moment, we do not have enough information to identify the exact structure and composition of the monomers although it is sure that $Cd(CH_3)_2$ cannot be the dominant Cd monomers (see below). In this paper, if it is not specified, monomers mean any molecular species, excluding nanocrystals, containing Cd and/or Se atoms.

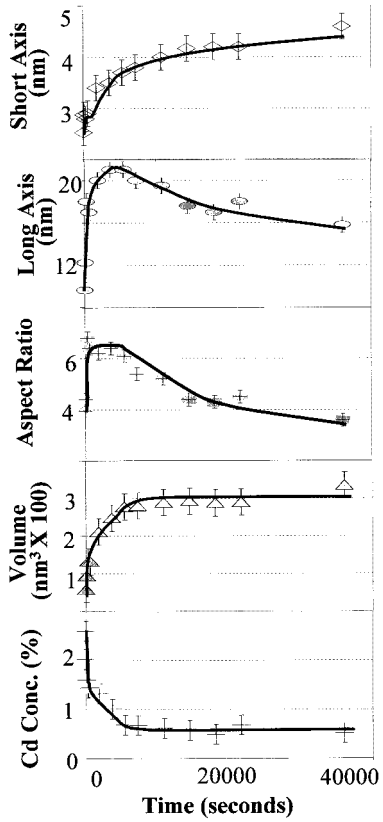

Figure 1. The temporal shape evolution of CdSe nanocrystals determined by TEM and the corresponding temporal variation of Cd monomer concentration in solution determined by ICP. In this specific synthesis, the HPA/TOPO mixture (8% HPA) was heated to 360 °C for the injection. The growth temperature was 250 °C. The Cd to Se atomic ratio was 1 to 1.3.

We found that the accuracy of this indirect Cd analysis largely depends on the actual amount of the aliquots taken from the reaction flask. When Peng et al.[26] developed the indirect method for measuring the monomer concentration, the volume of the aliquots was used as the standard. Due to the large temperature difference between the reaction mixture and the syringe, we found that it is very difficult to accurately measure the aliquot volumes. We found that measuring the mass of the aliquots added into methanol gives very reproducible and reliable data. We also observed that measuring the number of Cd atoms by ICP directly is more accurate than only weighing the mass of the dried CdSe nanocrystals purified from aliquots. The latter, adopted by Peng et al. in its original form for the indirect method for determining the monomer concentration, [26] has to assume a certain number and composition of the ligands on the surface of nanocrystals.

A typical temporal shape evolution of CdSe quantum rods occurs in three distinguishable stages. For the growth reaction corresponding to Figure 1, when the Cd monomer concentration in the solution was between 1.4% and 2% of cadmium element by mass, all the nanocrystals grew almost exclusively along their long axis and both aspect ratio and volume of crystals increased rapidly. Henceforth, we will refer to this stage as "exclusive 1-dimensional growth", or the "1D-growth stage".

The second stage of the example presented in Figure 1 occurred when the Cd monomer concentration dropped to between 0.5% and 1.4%. In this stage, crystals grew simultaneously in three dimensions. The aspect ratio remained constant, but the crystal volume increased. Henceforth, we will refer to this stage as "3-dimensional growth", or the "3D-growth stage".

It should be mentioned that this stage was not observed by Peng et al.,[1] probably because of the higher growth rates in their studies.

In the final stage of the example illustrated in Figure 1, when the Cd concentration was constant at 0.5%, the aspect ratio dropped noticeably, because the dimension of the crystals increased along the short axis and decreased along the long axis. Nanocrystal volumes and number remained constant, and there was no noticeable net growth or net dissolution of nanocrystals. This indicates that the monomers very likely moved on the surface of a crystal from one dimension (*c*-axis) to the other two dimensions in an intraparticle manner. Henceforth, we shall refer to this state as "1-dimension to 2-dimension intraparticle ripening", or "1D-to-2D-ripening". In the 1D-to-2D-ripening process, the quantum rods can eventually evolve to dot shape, if given enough time. This shape-evolution process, from rods to dots, was observed by Peng et al.,[1] although their results did not reveal the intraparticle diffusion feature. It should be mentioned that, for normal Ostwald ripening (interparticle ripening),[12] the Cd monomer concentration was determined to be only about 0.1−0.2% in this system.

In Figure 1, the 3D-growth and the 1D-to-2D-ripening stages were both quite obvious. However, the 1D-growth stage occurred over a short period of time. To confirm this stage, we carried out a reaction whose monomer concentration was maintained in the corresponding 1D-growth range for a longer time by the addition of more monomers to the reaction system at certain time intervals. In the experiment illustrated in Figure 2, the 1D-growth stage was successfully extended for about 4 h. The long axis of the quantum rods increased from about 35 nm (Figure 2a) to over 100 nm (Figure 2c) by the secondary injections, but the short axis remained almost constant, about 3−4 nm. The growth rate along the long axis was at least 2 orders of magnitude faster than that along the short axis.

The growth of quantum rods can start from the dot shape. Figure 3 demonstrates that nanocrystals were altered from close to monodisperse dots to nearly monodisperse quantum rods by significantly boosting the monomer concentration. Quantum rods formed by the use of monodisperse dots as "seeds" normally have better distribution for both short axis and the aspect ratio (see Figure 3 as an example).

For a larger short axis dimension, all stages require relatively lower monomer concentrations. For example, with 1% initial Cd concentration, the system cannot form the quantum rods with the same short axis dimension as shown in Figure 1, because this monomer concentration is in the 3D-growth stage of the experiment shown in Figure 1. In reality, the reaction yielded much thicker rods (short axis around 5 nm) right after the injection, and then those quantum rods evolved in similar three stages shown in Figure 1.

Type and concentration of the strong Cd ligands added play a very important role in determining the growth rate. In the example shown in Figure 3, it took about 23 h for the long axis dimension of the rods growing from about 8 nm (Figure 3b) to 20 nm (Figure 3c) using TDPA as the strong ligands. In general, the growth rate in TDPA/TOPO is magnitudes slower than that in the HPA/TOPO case. Furthermore, the growth of rods in TDPA/TOPO requires higher monomer concentrations. For instance, replacing TDAP by HPA in the example shown in Figure 3, the reaction forms rods almost instantly after the initial injection.

We found that neither the concentration of the strong ligands (HPA or TDPA) nor the strong ligand-to-Cd ratio in the mother solution was the determining factor for the crystal structure and the shape of nanocrystals. Quantum rods grown in either HPA or TDPA mixed with TOPO are all wurtzite crystals with the *c*-axis as the long axis (Figure 3d). A 1% concentration of HPA was too low to yield quantum rods with the initial monomer concentration reported by Peng et al. (0.7% Se and 1.4% Cd).[1] However, with the same HPA concentration, we synthesized quantum rods with a much higher monomer concentration (1.5% Se and 2.2% Cd). Even in the absence of a strong ligand, we observed the formation of nanorods with high monomer concentrations, although the short axis of these nanorods was larger than 10 nm immediately after the injection and those rods cannot be considered to be quantum rods.

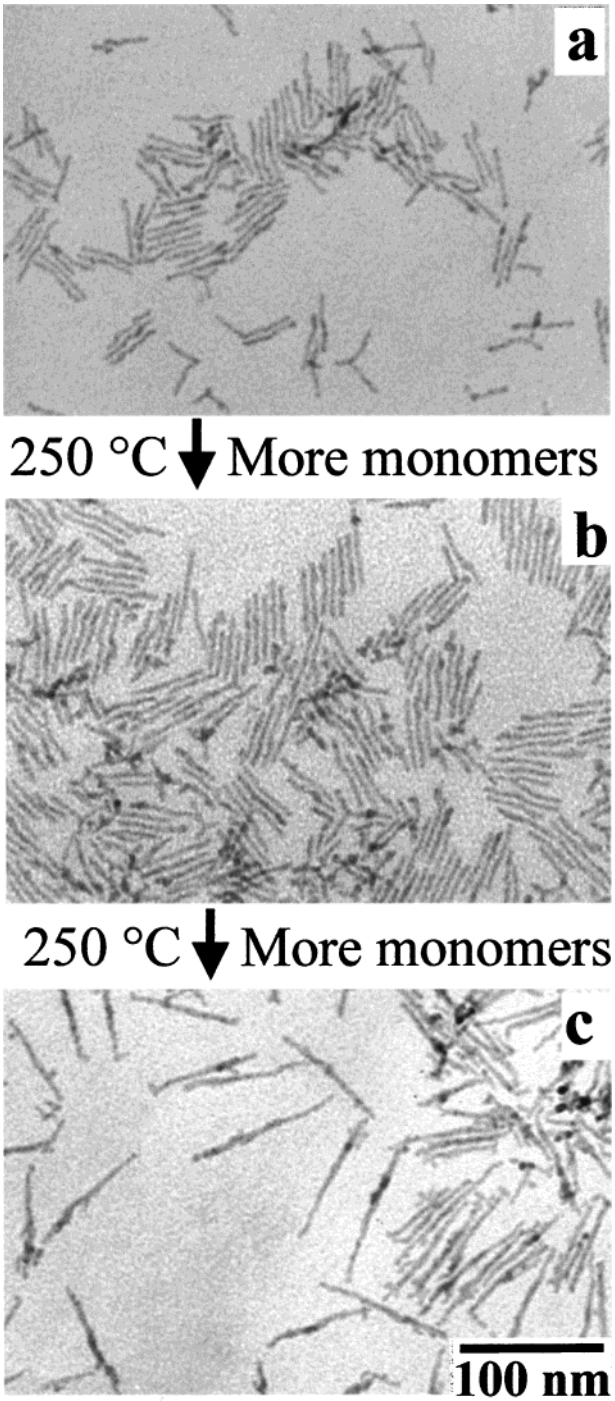

Figure 2. The extension of the 1D-growth stage by maintaining the monomer concentration in the right range. See the typical synthesis for the two-stock solution approach described in the Experimental Section for experimental details.

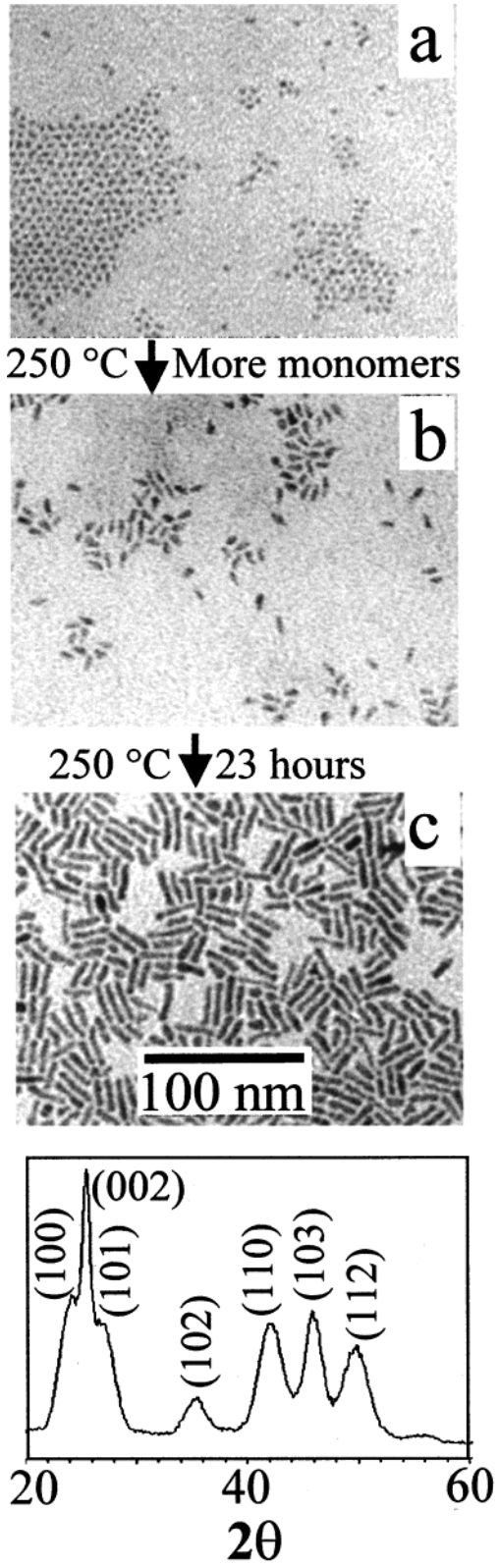

Figure 3. (a) Relatively monodisperse CdSe dots formed in 13% TDPA at 360 °C for injection and 250 °C for growth; (b and c), relatively monodisperse quantum rods grown from the dots in part a by a secondary injection and consequent growth for 23 h. Two grams of the primary stock solution ($Se:Cd(CH_3)_2$:TPB = 1.3:1.8:25 by mass) and 0.8 g of the secondary stock solution ($Se:Cd(CH_3)_2$:TPB = 1:1.8:15 by mass) were used for the initial and the second injections, respectively; (d) the XRD pattern of rods shown in part c.

The reaction initiated by the two-stock-solution approach can further clarify the role of the strong ligands. The Cd stock solution, $Cd(CH_3)_2$ dissolved in a small amount of TBP, was slowly dropped into the hot mixture of TOPO and HPA or TDPA. Ten to sixty seconds later, the Se stock solution of Se dissolved in TBP was rapidly injected. If the strong ligand-to-Cd mole ratio was smaller than 1, a yellowish-gray precipitate was observed immediately after the addition of $Cd(CH_3)_2$ stock solution. This yellowish-gray precipitate did not disappear after the injection of Se stock solution and it is suspected of being a cadmium metal precipitate.

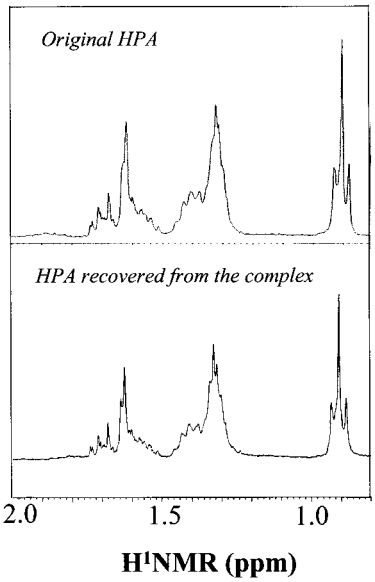

Figure 4. Proton NMR spectra of HPA. (Top) Original HPA added in the reaction vessel. (Bottom) HPA from the Cd−HPA complex recovered by the digestion and extraction (see Experimental Section for details).

If the strong ligand-to-Cd mole ratio was higher than 1, a colorless solution was obtained after the injection of the Cd stock solution and the consequent injection of Se stock solution generated nanocrystals (see Figure 2). The temporal evolution of these nanocrystals followed the same pattern as that of the one-stock-solution approach. The reaction initiated by the two-stock-solution approach was more reproducible than ones initiated by the single-stock solution containing both Cd and Se precursors. The two-stock-solution approach can also generate longer and relatively monodisperse quantum rods. In fact, we found that multiple injections with the one-stock-solution approach can only generate long rods mixed with significant amount of dots and short rods.

A white precipitate which is barely soluble in either toluene or methanol can be readily isolated in the early aliquots when strong ligands are used, regardless of the injection manner. For the two-stock-solution approach, if the strong ligand-to-Cd molar ratio is greater than 1, a large amount of the same precipitate in methanol is obtained from the colorless aliquots taken before the injection of the Se stock solution. These solubility characteristics are identical with that of the Cd−HPA complex synthesized by the reaction of HPA with $CdCl_2$. There are some subtle solubility differences between the complexes generated with different strong ligand-to-cadmium mole ratios. If this ratio is higher than 2, the precipitation finishes almost instantly after the aliquots are added into methanol. If the ratio is larger than 1 but smaller than 2, the white precipitate generates slowly from the clear methanol solution of the reaction mixture. This slow precipitation can take hours, and centrifugation/decantation at the early stage cannot either accelerate or stop this slow process.

Proton NMR (Figure 4) and mass spectroscopy reveal that

the organic component of the white precipitate after the digestion (see the isolation procedure in the Experimental Section) is identical to the starting strong ligands, either TDPA or HPA. The cadmium content of the aqueous phase of the digestion solution was determined by ICP. The HPA- or TDPA-to-cadmium mole ratio obtained by the above analysis is close to 2:1. NMR, mass spectroscopy and ICP measurements do not show any significant difference between the final precipitate generated with different initial strong ligand-to-cadmium mole ratios. However, the growth rate of rods with the HPA- or TDPA-to-cadmium ratio higher than 2 is significantly faster, implying the structural difference of the solution species. It should be mentioned that we did not observe any evidence of TOPO in the complex precipitated from methanol, although TOPO may somewhat play a role in the formation of Cd complex, especially in the case of the strong ligand-to-cadmium ratio between 1 and 2.

Discussion

The experimental results suggest that the strong Cd ligands do not directly affect the shape of the nanocrystals. However, it is clear that the strong ligands, either HPA or TDPA, are needed in the system to form a stable complex with cadmium (Cd−HPA or Cd−TDPA). Without strong ligands, it is impossible to maintain the high monomer concentration needed for the growth of quantum rods, because $Cd(CH_3)_2$ immediately decomposes at high temperatures and generates cadmium precipitate in pure TOPO. The experimental results suggested that, if the strong ligand-to-cadmium mole ratio is higher than 2, the composition of the complex is one cadmium coordinated with two HPA or TDPA molecules. In the case of the strong ligand-to-cadmium mole ratio lower than 2 but higher than 1, the ligands for the complex are likely a mixture of the strong ligand added and TOPO. In methanol, this Cd complex is not as stable as the complex for Cd coordinated only by HPA or TDPA, and it decomposes slowly and gradually in methanol.

For typical crystal growth in solution, two processes occur in sequence. At first, monomers diffuse from bulk solution and approach the area right next to the surface of a crystal (stagnant solution), then they react with the surface of the crystal. The experimental results described above strongly suggest that the growth of CdSe quantum rods and quantum dots under current conditions is a diffusion-controlled process, instead of a reaction-controlled process, based on the following arguments.

If the growth reaction is the controlling step, the monomer concentration in the stagnant solution is equal to the monomer concentration in the bulk solution. The growth rate of each facet depends on its surface area and reactivity. In principle, if the monomer concentration is higher than the solubility of a given facet, that facet should grow at a rate proportional to the monomer concentration in solution.[12] Apparently, this is not the case for the growth process described here. For instance, reaction-controlled growth cannot explain why the short axis remains constant at high monomer concentration in the 1D-growth stage but grows visibly at lower concentrations in the 3D-growth and the 1D-to-2D-ripening stages (Figure 1).

For diffusion-controlled crystal growth, each crystal is surrounded by a diffusion sphere. The monomer concentration gradient between the bulk solution and the stagnant solution as well as the diffusion coefficient of the monomers determine the direction (out or into the diffusion sphere) and the diffusion flux. The monomer concentration in the stagnant solution maintains the solubility of a given facet by the rapid growth onto or dissolution from the facet.[12] All the experimental results observed are consistent with diffusion-controlled growth. For instance, the longer hydrocarbon chain of TDPA resulted in a slower reaction rate, because of the smaller diffusion coefficient of the Cd−TDPA complex. This smaller diffusion coefficient consequently should require a higher monomer concentration in the bulk solution to maintain the same diffusion flux of monomers. This explains why, with the same monomer concentration in the bulk solution, the reaction may generate dots with TDPA/TOPO while it can yield quantum rods in HPA/TOPO. Certainly, the growth of CdSe quantum dots in the same solvent system should also be diffusion controlled since the monomer concentration in the bulk solution and the monomer concentration gradient is even lower than that in the 1D-to-2D-ripening stage. Therefore, the focusing of size distribution observed [26] should be a result of diffusion control, and may not be due to the high growth reactivity of the smaller nanocrystals in the solution.

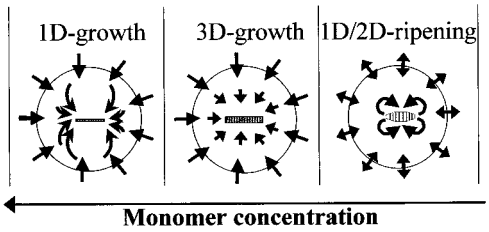

Figure 5. A schematic diagram for the proposed mechanisms of the three stages of the shape evolution. The circle in each stage is the interface between the bulk solution and the diffusion sphere. Arrows indicate the diffusion directions of the monomers. The double-directed arrows represent the diffusion equilibrium in the 1D-to-2D-ripening stage.

The thickness of the diffusion sphere can be determined by the growth kinetics data. A simple calculation using the data reported previously[26] reveals that the size of the quantum dots is negligible compared to the thickness of the diffusion sphere. This is actually very common for a diffusion-controlled growth process.[12] This fact means diffusion-controlled growth of nanocrystals is significantly different from the synthesis of nanocrystals in reverse micelle whose dimension can be just slightly larger than the nanocrystal formed inside.[18]

Apparently, the kinetically controlled shape evolution discussed here cannot be explained by the Gibbs−Curie−Wulff law,[12] which predicts that the shape of a crystal is thermodynamically determined by the relative chemical potential of all the possible facets and does not allow any shape evolution. With the experimental results discussed above, the mechanisms (Figure 5) of the shape evolution are deduced as follows.

At high temperatures, CdSe grows in the wurtzite (hexagonal) structure (see Figure 3d). A dipole moment of CdSe nanocrystals along this axis was reported.[28] In the stable form shown on the left of Figure 6, all the atoms on both facets perpendicular to the *c*-axis (unique facets) have only one dangling bond without surface reconstruction. The facets terminated by negatively charged Se atoms and positively charged Cd atoms are the (00$\bar{1}$) facet and (001) facet, respectively. The negatively charged (00$\bar{1}$) facet is more or less uncoated, because the ligands in the solution are all electron-donating ligands and should bind exclusively to cationic species. Additionally, without surface reconstructions, any surface Cd atom grown on the (00$\bar{1}$) facet has to possess three dangling bonds, even if the surface Cd atoms reach a full monolayer. These unique structural features of the (00$\bar{1}$) facet and the dipole moment along the *c*-axis significantly increase

(28) Blanton, S. A.; Leheny, R. L.; Hines, M. A.; Guyot−Sionnest, P. *Phys. Rev. Lett.* **1997**, *79*, 865.

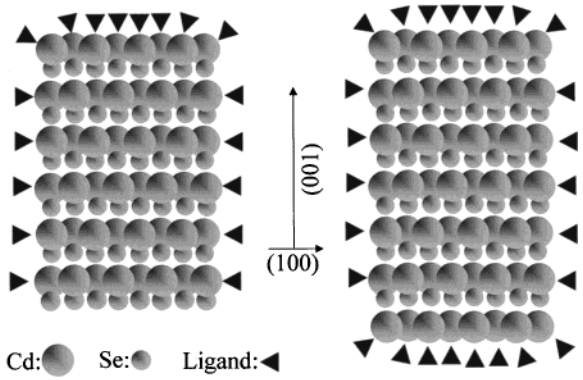

Figure 6. Schematic structure of CdSe quantum rods in growth. The most stable form of a rod is shown on the left, its (00$\underline{1}$) facet terminated by Se atoms does not have any ligand on it. After growing a monolayer of Cd atoms on the (00$\underline{1}$) (right), this facet is still relatively active compared to the other facets, because the surface Cd atoms on this facet have three dangling bonds. See text for more details.

the chemical potential of the unique facets, especially the (00$\underline{1}$) facet, compared to the others.

In the 1D-growth stage, when the monomer concentration in the bulk solution is high, the chemical potential of the monomers in the bulk solution is significantly higher than that in the stagnant solution at any facets of the crystals. This means that monomers should diffuse into the diffusion sphere (Figure 5). As a result, the volume of nanocrystals increases noticeably (see Figure 1). However, the unique structural feature of the (00$\underline{1}$) facet and the high chemical potential on both unique facets makes the growth reaction rate along the *c*-axis much faster than that along any other axis. The limited amount of monomers maintained by diffusion is mainly consumed by the quick growth of the unique facets, especially the (00$\underline{1}$) facet. As a result, the diffusion flux goes to the *c*-axis exclusively and makes the unique axis the long axis of the quantum rods. In this specific stage, the reactivity of different facets plays an important role. However, this stage is still diffusion controlled because the diffusion flux is only enough for the quick growth along the unique axis.

When the monomer concentration drops to a certain level, the overall chemical potential gradient between the bulk solution and the different facets decreases. The growth slows down, with slower crystal volume increases as an indicator, compared to the 1D-growth (see Figure 1). However, this gradient drop impacts the unique facets the most, because of their relatively high chemical potential compared to the other facets. The smaller gradient between the stagnant solution of the unique facets and the bulk solution makes the diffusion flux difficult to go to in the unique facets. The high growth reaction rate and small diffusion driving force along the unique axis somewhat cancel each other. As a result, the monomers entering the diffusion sphere are shared by all three dimensions. This is the 3D-growth.

In the 1D-to-2D-ripening stage, the chemical potential of the monomers in the bulk solution drops to lower than the chemical potential of the two unique facets, but higher than that of the others. Overall, the chemical potential in the bulk solution approximately equals the average chemical potential of the entire surface atoms of a nanocrystal. This leads to a diffusion equilibrium on the interface of the diffusion sphere. This is why both the volume of nanocrystals and the monomer concentration in the bulk solution remain constant. Without incoming diffusion flux, the monomers start to diffuse from the stagnant solution of the unique facets to the stagnant solution of the other facets, because of the internal chemical potential gradient. Consequently, atoms on the unique facets dissolve into their stagnant solution to maintain the solubility equilibrium. The same equilibrium drives the other facets to take monomers from their stagnant solution. The net result is that the atoms on the two unique facets move to the other facets in an intraparticle manner.

As mentioned above, the interparticle Ostwald ripening occurs at a monomer concentration several times lower than this intraparticle ripening. This fact implies that the existence of the 1D-to-2D-ripening is due to the extremely high overall chemical potential of the rod shape. When the crystals reach their equilibrium shape required by the Gibbs−Curie−Wulff law,[12] the intraparticle ripening should stop. Apparently, such an intraparticle ripening process may occur for any thermodynamic metastable shape under adequate chemical environments. Intraparticle diffusion cannot happen in the 1D-growth stage and the 3D-growth stage because the incoming diffusion flux from the bulk solution efficiently suppresses the intraparticle migration of monomers.

The growth of quantum dots requires monomer concentrations even lower than the 1D-to-2D-ripening stage. Crystals should take the thermodynamic shape predicted by the Gibbs−Curie−Wulff law, because the monomers can readily diffuse around crystals at any moment. This means that diffusion-controlled growth can produce nanocrystals with Wulff facets as observed.[29]

It should be pointed out that the preferential binding of the ligands to cationic sites on the surface of nanocrystals plays an important role in this model. However, most experimental results presented here, especially the evolution of the shape of nanocrystals, cannot be explained only based on this preferential binding.

Conclusion

This paper demonstrated that shape evolution of colloidal nanocrystals can be fully accessed experimentally. Since the solubility/chemical potential of nanocrystals is strongly dependent upon their size and shape,[12] a reasonably good distribution of nanocrystals is essential for the study. Such experiments provide unique and convincing information for understanding the growth mechanisms of shape-controlled nanocrystals. The results demonstrate that a diffusion-controlled growth process can generate shape-controlled nanocrystals. As a sensitive indicator, shape evolution uncovers many insights for the formation of nanocrystals in general. These types of experiments shed new light on the understanding of crystallization in general. This will further impact many fields related to crystallization and crystal growth. In fact, the growth mechanisms revealed by this study has already been used for designing a new synthetic scheme for high quality cadmium chalcogenides nanocrystals using CdO as the cadmium precursor.[30]

Acknowledgment. This work is supported by the University of Arkansas through the startup funds and by the Quantum Dots Incorporation, CA.

Supporting Information Available: Hi-resolution TEM picture of CdSe quantum rods and isolation and analysis of the Cd-HPA complex (PDF). This material is available free of charge via the Internet at http://pubs.acs.org.

JA0027766

(29) Shiang, J. J.; Kadavanich, A.; Alivisatos, A. P. *J. Phys. Chem.* **1995**, *99*, 17417−17422.
(30) Peng, Z. A.; Peng, X. *J. Am. Chem. Soc.* **2001**, *123*, 183−184.